ORIGINAL RESEARCH

The Bi-steric Inhibitor RMC-5552 Reduces mTORC1 Signaling and Growth in Lymphangioleiomyomatosis

Jilly F. Evans[1,2*], Owen A. Ledwell[1,2*], Yan Tang[3], Ryan Rue[1,2], Alexander R. Mukhitov[1,2], Rémi Diesler[4,5], Susan M. Lin[1,2], Swaroop V. Kanth[1,2], Maria C. Basil[1,2,3], Edward Cantu[3], Elizabeth P. Henske[4], and Vera P. Krymskaya[1,2]

[1]Division of Pulmonary, Allergy, and Critical Care Medicine, Department of Medicine, [2]Lung Biology Institute, Perelman School of Medicine, and [3]Division of Cardiovascular Surgery, University of Pennsylvania, Philadelphia, Pennsylvania; [4]Division of Pulmonary and Critical Care Medicine, Department of Medicine, Brigham and Women's Hospital and Harvard Medical School, Boston, Massachusetts; [5]Department of Respiratory Medicine, National Reference Centre for Rare Pulmonary Diseases, Hospices Civils de Lyon, Université Lyon 1, UMR754, INRAE, ERN-LUNG, Lyon, France

ORCID IDs: 0000-0001-6443-0788 (A.R.M.); 0000-0003-0746-357X (R.D.); 0000-0003-4716-1285 (M.C.B.); 0000-0003-1105-0129 (E.C.); 0000-0002-0584-4486 (V.P.K.).

Abstract

Mutations in the TSC (tuberous sclerosis complex) genes result in the hyperactivation of the mTORC1 (mechanistic/mammalian target of rapamycin 1) growth pathway in mesenchymal pulmonary cells. Rapamycin (sirolimus), a naturally occurring macrolide, is the only therapeutic approved for women with lymphangioleiomyomatosis (LAM), a progressive, destructive lung disease caused by TSC gene mutations and mTORC1 hyperactivation. However, on cessation of the drug, lung function decline continues. We demonstrated here that pulmonary LAM cancer stem-like state (SLS) cells most highly expressed the eIF4E (eukaryotic translation initiation factor 4E)-dependent translation initiation genes. We also showed that the 4E-BP1 (eukaryotic initiation factor 4E-binding protein 1) gene has the lowest expression in these cells, indicating that the 4E-BP1/eIF4E ratio in LAM SLS cells favors unrestrained eIF4E oncogenic mRNA translation. The bi-steric mTORC1-selective compound RMC-5552 prevented growth of LAM-associated fibroblasts and phosphorylation of proteins in the ribosomal protein S6K1/ribosomal protein S6 (S6K1/S6) and 4E-BP1/eIF4E translation mTORC1-driven pathways, whereas rapamycin only blocked the S6K/S6 axis. Rapamycin inhibition of LAM-associated fibroblast growth was rapidly reversed, but RMC-5552 inhibition was more durable. RMC-5552, through its potential to eradicate LAM cancer SLS cells, may have therapeutic benefit in LAM and other diseases with mTORC1 hyperactivity.

Keywords: lymphangioleiomyomatosis; TSC2; mTORC1; rapamycin; RMC-5552 bi-steric inhibitor

Mutations in the TSC (tuberous sclerosis complex) suppressor genes, TSC1 (hamartin) and TSC2 (tuberin), result in the hyperactivation of the mTORC1 (mechanistic/mammalian target of rapamycin 1) complex, which activates a major cellular growth and proliferation pathway (1, 2). In human lymphangioleiomyomatosis (LAM) disease, LAM cells cause progressive cystic lung destruction, resulting in the loss of lung function, especially in premenopausal women and during pregnancy (3). LAM cells have reemerged in donor lungs after lung transplantation,

(Received in original form May 24, 2024; accepted in final form ■■■)

*These authors contributed equally to this work.

Supported by National Institutes of Health/National Heart, Lung, and Blood Institute Clinical Center grants R01HL151467 (V.P.K.), RO1HL158737 (V.P.K.), RO1 UO1 HL131022 (L.P.H., V.P.K.), and RO1HL155821 (E.C.).

Author Contributions: J.F.E. conceived the project, performed experiments, and co-wrote the manuscript. O.A.L. performed experiments, prepared the figures, and co-wrote the manuscript. Y.T. performed single-cell RNA-sequencing data analyses. R.R., A.R.M., R.D., S.M.L., and S.V.K. performed experiments. M.C.B. and E.C. provided normal lung tissues. E.P.H. and V.P.K. funded the project and reviewed and revised the paper. All authors reviewed and approved the final version of the manuscript.

Correspondence and requests for reprints should be addressed to Jilly Evans, Ph.D., Pulmonary, Allergy, and Critical Care Division, Penn Center for Pulmonary Biology, University of Pennsylvania Perelman School of Medicine, Stemmler Hall, 2nd Floor, Suite 216, 3450 Hamilton Walk, Philadelphia, PA 19104. E-mail: jillyfevans@gmail.com.

This article has a data supplement, which is accessible at the Supplements tab.

Am J Respir Cell Mol Biol Vol ■■, Iss ■■, pp 1–10, ■■ ■■ 2024

Originally Published in Press as DOI: 10.1165/rcmb.2024-0242OC on ■■■
Internet address: www.atsjournals.org

Clinical Relevance

Rapamycin, the only therapeutic approved for lymphangioleiomyomatosis (LAM), does not block mTORC1 (mechanistic/mammalian target of rapamycin 1)-induced eIF4E (eukaryotic translation initiation factor 4E)-dependent oncogenic translation initiation. We show here that the eIF4E initiation translation proteins are selectively expressed in LAM cancer stem-like cells. The bi-steric mTORC1-selective inhibitor RMC-5552 inhibits LAM-associated fibroblast growth and signaling more durably than rapamycin. RMC-5552 has the potential to eradicate LAM stem-like cells and therefore be a longer-lasting therapy than rapamycin is for LAM.

demonstrating that LAM has the features of a slowly progressing metastatic neoplasm (4, 5). Through an outstanding collaboration of scientists, clinicians, and patients, rapamycin (sirolimus), an allosteric inhibitor of mTORC1, was shown to inhibit LAM progression in many patients, but the mechanism of inhibition is cytostatic, not cytotoxic, so on cessation of the drug the disease progression continues (3, 5).

The TOR kinase is a serine/threonine kinase that is central to two structurally and functionally distinct complexes, namely mTORC1 and mTORC2, and phosphorylates more than 100 different protein substrates (6). Several subunits are expressed in both mTOR complexes, but the proteins Raptor and Rictor are uniquely expressed in mTORC1 and mTORC2, respectively (6). TSC controls mTORC1 activity, acting as a rheostat of external environmental growth factors and nutrients to accelerate anabolic protein, nucleotide, and lipid synthesis and decrease catabolic autophagy (7). First-generation mTORC1 inhibitors, referred to as rapalogs, are close analogs of rapamycin. These compounds inhibit phosphorylation of many mTORC1 substrates but do not acutely inhibit any mTORC2 substrates (6). mTORC1 controls protein synthesis via the ribosomal protein S6K1/S6 axis and the 4E-BP1/eIF4E (eukaryotic initiation factor 4E-binding protein 1/eukaryotic translation initiation factor 4E) axis (7) (*see* Figures E1A and E1C in the data supplement). Phosphorylation of S6K by mTORC1 primarily controls ribosomal synthesis, whereas phosphorylation of 4E-BP1 enables the release of the rate-limiting, mRNA cap-binding eIF4E translation initiation factor, which selectively drives translation of proliferative, antiapoptotic, angiogenic, and stem cell survival genes (8). Nonphosphorylated 4E-BP1 and eIF4E have been shown to be expressed in both nuclear and cytoplasmic cellular locations (9). mTORC1 phosphorylation proceeds sequentially, with the initial phosphorylation of 4E-BP1 at threonines 37 and 46 being sufficient for the release of eIF4E (10, 11). Rapamycin inhibits the phosphorylation of S6K1/S6; although it does not inhibit the initial phosphorylation of the threonine 37 and 46 4E-BP1 sites, it can inhibit phosphorylation on 4E-BP1 serine 65 and threonine 70, but these dephosphorylations do not affect eIF4E release (11).

Second-generation mTOR inhibitors directly inhibit the mTOR kinase ATP-binding active site, thereby blocking both mTORC1 and mTORC2 activity. These compounds and dual mTOR kinase/PI3K inhibitors prevent phosphorylation of both the S6K1/S6 and 4E-BP1 translation axes (12, 13). However, these ATP-competitive compounds have adverse effects associated with their use, partly through their inhibition of mTORC2 (13, 14). For example, the inhibition of mTORC2 activity in the liver results in hyperglycemia that may result in insulin tolerance and could contribute to metabolic disorders (14). Most importantly, the considerable clinical side-effect profiles of second-generation mTOR kinase inhibitors makes them incompatible with chronic dosing in patients with LAM.

Third-generation mTORC1 bi-steric inhibitors were developed by joining rapamycin through an extended variable size linker to an active site TOR kinase inhibitor (15–18) (Figure E1B). These bi-steric mTORC1 inhibitors block both mTORC1 protein translation nodes (15–18). The bi-steric inhibitors RMC-6272 and RMC-4627 were shown to inhibit *in vitro* growth of cancer cells and tumors with mTORC1 hyperactivation in a *tour de force* by Du and colleagues (19). These two compounds, and in addition RMC-5552, prevented patient-derived tumor xenograft growth *in vivo* (19). All bi-steric compounds are more potent against mTORC1 than mTORC2, with RMC-5552 being the most selective (>40-fold selectivity for mTORC1 vs. mTORC2) (19) (Figure E1D). Bi-steric inhibitors exhibited both cytostatic and cytotoxic mechanisms, including blocking cell cycling and inducing apoptosis (19, 20). The importance of blocking the 4E-BP1/eIF4E pathway in cancer was highlighted by a reverse-phase protein assay of patient samples from 31 tumor types that demonstrated that p4E-BP1 and mTOR activity, but not pS6K activity, was associated with poor prognosis (19).

Several independent groups have performed single-cell RNA sequencing (scRNA-seq) analysis of LAM lung and have identified very similar, but not identical, small unique subsets of cells that express LAM biomarker genes, extracellular matrix (ECM) remodeling genes, WNT growth pathway genes, and urogenital genes (21–23). The data from these analyses are available at the LAM Atlas site (24). Tang and colleagues also performed scRNA-seq on six renal angiomyolipomas (AML) (23). AML are distinctive benign tumors that occur in at least 50% of women with LAM. Unique specific cells, identified in Tang and colleagues (23), in both LAM lung and renal AML, were clustered into distinct cell states based on expression of 55 known cancer stem cell genes defined by CancerSEA analysis (25) (Table E1). Based on the expression of these genes, LAM cells were termed "stem-like state" (SLS), with abundant cancer stemness and dormancy-related genes, and those with fewer cancer stemness genes and more inflammatory cytokine and chemokine genes were termed an "inflammatory state" (IS) and an intermediate state (23).

Because rapamycin is the only U.S. Food and Drug Administration–approved therapy for LAM, but does not inhibit eIF4E-dependent translation, we evaluated the inhibition of growth and mTOR signaling in fibroblasts by the bi-steric mTORC1 inhibitor RMC-5552 (Figure E1B). RMC-5552 is the only bi-steric compound in clinical studies, namely in phase 1 oncology trials (NCT047774952; NCT05557292). RMC-5552 was synthesized by covalently attaching rapamycin via a linker to the dual mTOR kinase inhibitor INK128 (MNL128, TAK-228, and Sapanisertib). RMC-5552 binds weakly to mTORC2, because Rictor partially occludes the FKBP12 binding site on mTOR (Figure E1D).

We hypothesized that bi-steric inhibitors might offer effective therapy for LAM because of their inhibition of the rapamycin-insensitive 4E-BP1/eIF4E-dependent oncogenic translation initiation pathway. We investigated the expression of the eIF4E pathway translation initiation genes in LAM-specific lung cells by analysis of scRNA-seq data previously deposited at Gene Expression Omnibus GSE190260 (23) and demonstrated the highest expression of these genes in SLS cells. We confirmed the heterogeneity of expression of markers of LAM cells and mTORC1 activation, namely α-SMA, PMEL, pS6, and p4E-BP1, in LAM lung lesions. In addition to cytoplasmic expression, we found intense nuclear immunofluorescence of p4E-BP1 in both LAM lung tissue and LAM-associated fibroblasts (LAFs). Importantly, we demonstrated durable and selective inhibition of growth and both mTORC1 translation signaling axes in LAFs by RMC-5552.

Methods

Human Lung Tissue

Normal lung samples were obtained from deidentified nonused lungs donated for organ transplantation following an established protocol (PROPEL), approved by University of Pennsylvania institutional review board. LAM lung samples were obtained from living donors undergoing transplantation through the National Disease Research Institute). Informed consent was obtained by National Disease Research Institute before acceptance of tissue donation. For both normal and diseased (LAM) lung samples, identifying information was removed before use in accordance with institutional and National Institutes of Health protocols.

Isolation of Fibroblasts and Cell Culture

Single-cell suspensions from human lung samples were prepared using previously described methods and used between passages 2 and 5 (22). Cells were grown in Dulbecco's modified Eagle medium, 100 U/ml penicillin, 100 μg/ml streptomycin, 10 mM glutamine, and 10% FBS, maintained at 37°C in 5% CO_2. Rapamycin (LCL), Torin 1 (Cayman Chemicals), INK128 (Cell Signaling), and RMC-5552 (MedChem Express) were made as DMSO stocks (1–100 mM) and stored at −20°C. For growth inhibition, normal human lung fibroblasts (NHLFs) and LAFs were seeded in 96-well plates at 3,000 cells/well, and for drug washout experiments in 6-well plates at 10,000 cells/well. Vehicle control was 0.1% DMSO. For growth inhibition experiments, baseline absorbance at 570 nm (A570 nm) (∼0.4) before drug addition was subtracted from final absorbances. Crystal violet staining monitored growth as described (13).

scRNA-Seq, Cancer Stemness Cell Clustering, and Data Processing

LAM lung samples were collected under institutional review board approval by the Brigham and Women's Hospital and processed as described (23). LAM-specific cells were clustered for cancer stemness based on expression of 55 cancer stem cell genes (25) (Table E1).

Lung and Cell Immunofluorescent Analyses

Human lung parenchymal tissue used for immunofluorescence analyses was processed as described (22). Primary antibodies were α-SMA (Sigma, A2547), pS6Ser 235/236 (#62016), Tsc2 (#4308), and p4E-BP1Thr 37/46 (#2855), all from Cell Signaling, and anti-PMEL from Dako (M0634). Secondary antibodies were Goat Anti-Rabbit Alexa Fluor 647 (ab150083) and Goat Anti-Mouse Alexa Fluor 488 (ab150113) from Abcam, except PMEL staining, where secondary was Goat Anti-Mouse Alexa Fluor 594 from Invitrogen (A11005). For *in vitro* studies, LAFs were fixed, incubated with antibodies for 1 hour at room temperature, stained with DAPI, washed, and embedded in ProLong Diamond embedding media. Visualization was with an Eclipse 2000 microscope (Nikon), except for PMEL, which used a Fluoview (Olympus) confocal microscope.

Cell Lysate Preparation and Immunoblotting

Cells were lysed and proteins were separated by SDS-PAGE and immunoblotted as described (13). Primary antibodies were pS6Ser240/244 (#5364), p4E-BP1Thr37/46 (#2855), pAktSer473 (#4060), pNDGR1Thr346 (#8947), S6 (#2217), 4E-BP1 (#9644), Akt (#9272), β-Actin (#4970), Tsc2 (#4308), and eIF4E (#9742), all from Cell Signaling, and anti-NDRGR1 antibody from ProteinTech (#26902). Antibodies were at 1:1,000, except β-Actin at 1:15,000. Washed blots were incubated for 1 hour at room temperature with 1:15,000 LiCor800CW secondary antibody and then analyzed on a LiCor Odyssey reader.

Statistical Analysis

Statistical differences were calculated using Graph Pad Prism version 10. Growth inhibition curves were produced using a variable slope (four parameter) nonlinear regression analysis initialized to mean of respective controls with a 95% confidence interval.

Results

eIF4E Translation Initiation Genes Are Expressed in LAM Cell Clusters with the Highest Expression of Cancer Stem-like Genes

Based on methodology from our earlier studies in the LAM lung (23), and scRNA-seq data deposited as Gene Expression Omnibus GSE190260, the presence of 55 cancer stemness genes defined previously (25) (Table E1) were identified in unique LAM cells in lung (23). Cells from five LAM lungs (57,186 cells total) were analyzed and, based on the presence of two or more of the LAM marker genes PMEL, MLANA, CTSK, VEGFD, and MITF, a total of 375 unique LAM cells were identified (23). In the unique LAM cells, "cancer stemness" gene expression from high to low was clustered into high (SLS), intermediate, and low (IS) states (23), as schematically shown in Figure 1A. We analyzed these clusters for the gene expression of EIF4EBP1, which codes for the 4E-BP1 protein, and EIF4E, EIF4A, and EIF4G, the proteins that comprise the cap-binding complex eIF4F (Figure E1C). EIF4EBP1 mRNA in LAM cells was most highly expressed in the intermediate stemness cell cluster and next highest in the low stemness IS cluster (Figure 1B). We demonstrated that the genes EIF4E, EIF4A1, and isomer EIF4A2 (not shown), EIF4G1, and isomers eIF4G2, eIF4G3 (not shown) were most highly expressed in the high and intermediate stemness clusters (Figures 1D and 1E). These gene-clustering data indicated that the 4E-BP1/eIF4E ratio in SLS LAM cells would favor the translation of eIF4E-dependent proteins and the potential for unrestrained translation of critical survival genes. It was previously suggested that the important factor determining activation of the translation initiation of oncogenic genes is the ratio of 4E-BP1/eIF4E (26). However, 4E-BPs may also play other roles in some cancers (27).

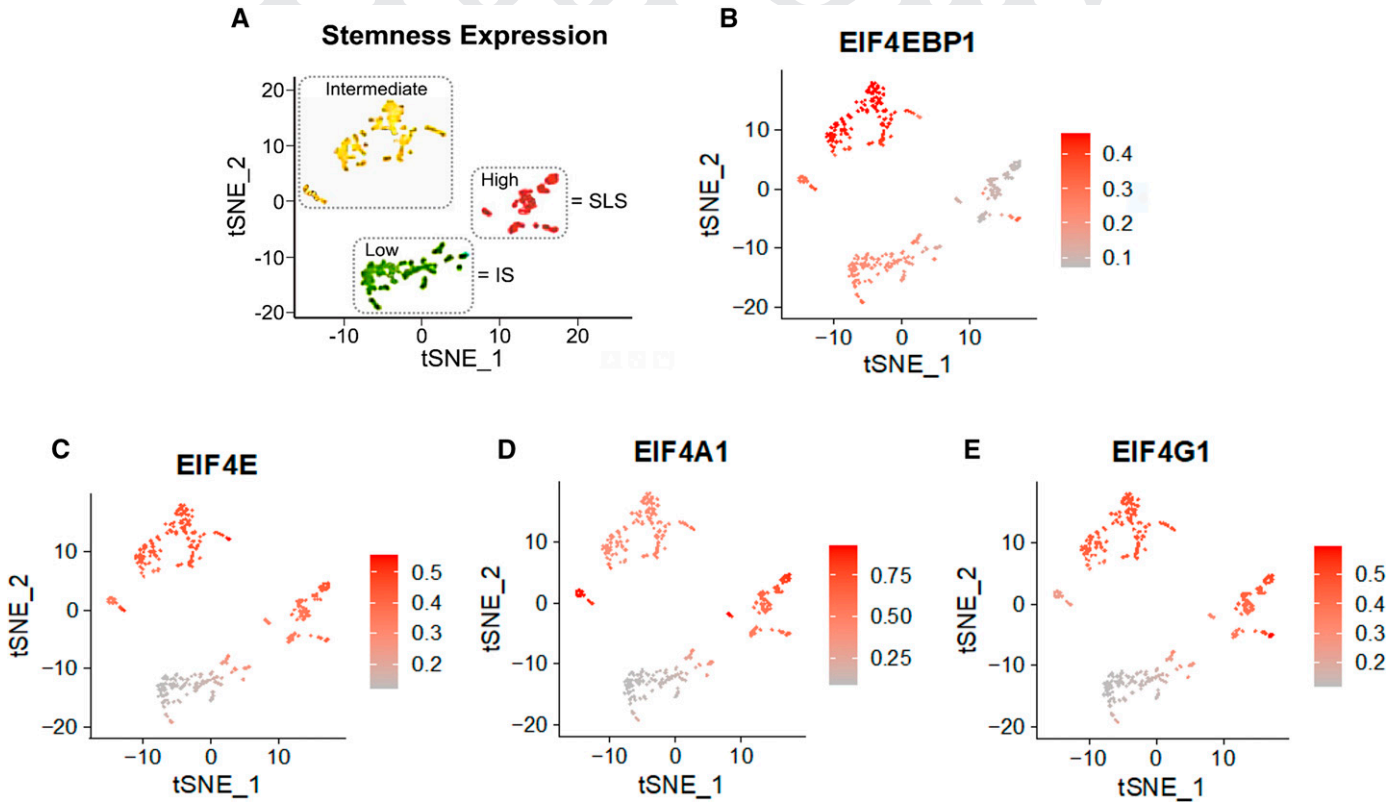

Figure 1. Elevated expression of genes associated with 4E-BP1/eIF4E (eukaryotic initiation factor 4E-binding protein 1/eukaryotic translation initiation factor 4E) translation initiation in the stem-like cells in lymphangioleiomyomatosis (LAM) lung. (*A*) Schematic of cancer cell stem-like status of LAM lung cells calculated based on the expression of 55 cancer cell stemness genes in CancerSEA (25) (Table E1). SLS = stem-like state (high stemness score, red), IS = inflammatory state (low stemness score, green), and intermediate state (yellow). (*B–E*) Expression of EIF4EBP1 (*B*), EIF4E (*C*), EIF4A1 (*D*), and EIF4G1 (*E*) in LAM cells. The quantification scale of red to gray indicates high to low of imputed normalized expression of genes as described (23).

18

Immunofluorescent Expression of pS6 and p4E-BP1 Proteins in Normal and LAM Lung

To highlight the activation of S6K1/S6 versus 4E-BP1/eIF4E in normal versus LAM lung parenchyma, we analyzed the expression of pS6 and p4E-BP1 compared with α-SMA (a myofibroblast marker), PMEL (HMB45) (a selective LAM cell marker) (28), and Tsc2/tuberin (Figure 2). Normal lung cells had low expression of pS6 or α-SMA (Figure 2A) in contrast to high expression in LAM lung lesions (Figure 2B). In LAM lung, there were areas of overlapping pS6 and α-SMA–positive cells, but some cells only showed α-SMA immunofluorescence, confirming not all LAM lesion myofibroblasts had hyperactivated mTORC1 (Figure 2B). Normal alveolar lung cells expressed Tsc2/tuberin protein but minimal pS6 (Figure 2C), as did stromal cells surrounding LAM lesions (Figure 2D), whereas within LAM nodules pS6 was strongly expressed with minimal expression of Tsc2/tuberin (Figure 2D). In another set of normal and LAM lungs, we studied the expression of the LAM cell marker PMEL (HMB45) (Figures 2E and 2F). The presence of melanoma markers in lung is atypical and is a diagnostic indicator of LAM. Normal alveolar lung cells showed only a background autofluorescent signal in the PMEL channel (Figure 2E), whereas LAM nodules had striking, but heterogeneous, PMEL immunofluorescence (Figure 2F). The single transmembrane PMEL protein had a granular cytoplasmic distribution consistent with expression in endoplasmic reticulum and Golgi body membranes and with previous immunoelectron microscopic studies showing PMEL in small granules resembling early-stage melanosomes (28). As expected, the stromal cells surrounding the LAM lesions were PMEL-negative (Figure 2F). In a third independent set of normal and LAM lung tissue samples, we demonstrated intense p4E-BP1 and pS6 in LAM lung in contrast to normal lung, except for autofluorescence generated by interstitial macrophages (Figures 2G–2J). The p4E-BP1 immunofluorescence was apparent in both nuclei and cytoplasm (Figure 2H), suggesting mTORC1 activity in the nucleus. Dual p4E-BP1 and pS6 immunofluorescence staining indicated modest expression of both proteins in normal lung, except for intense macrophage autofluorescence in the red channel (Figure 2K). By contrast, there was significant coexpression of pS6 and p4E-BP1 in some areas of LAM lung, again with nuclear and cytoplasmic expression of p4E-BP1 (Figure 2L). To the best of our knowledge, this is the first identification of p4E-BP1 in LAM cell nuclei.

Potent and Durable Inhibition of Fibroblast Growth by the Bi-steric mTORC1 Inhibitor RMC-5552

The number of unique LAM Tsc2-null lung cells may be <1% of total cells (23), and it has been very difficult to isolate and grow TSC-null LAM cells *in vitro*. Previous

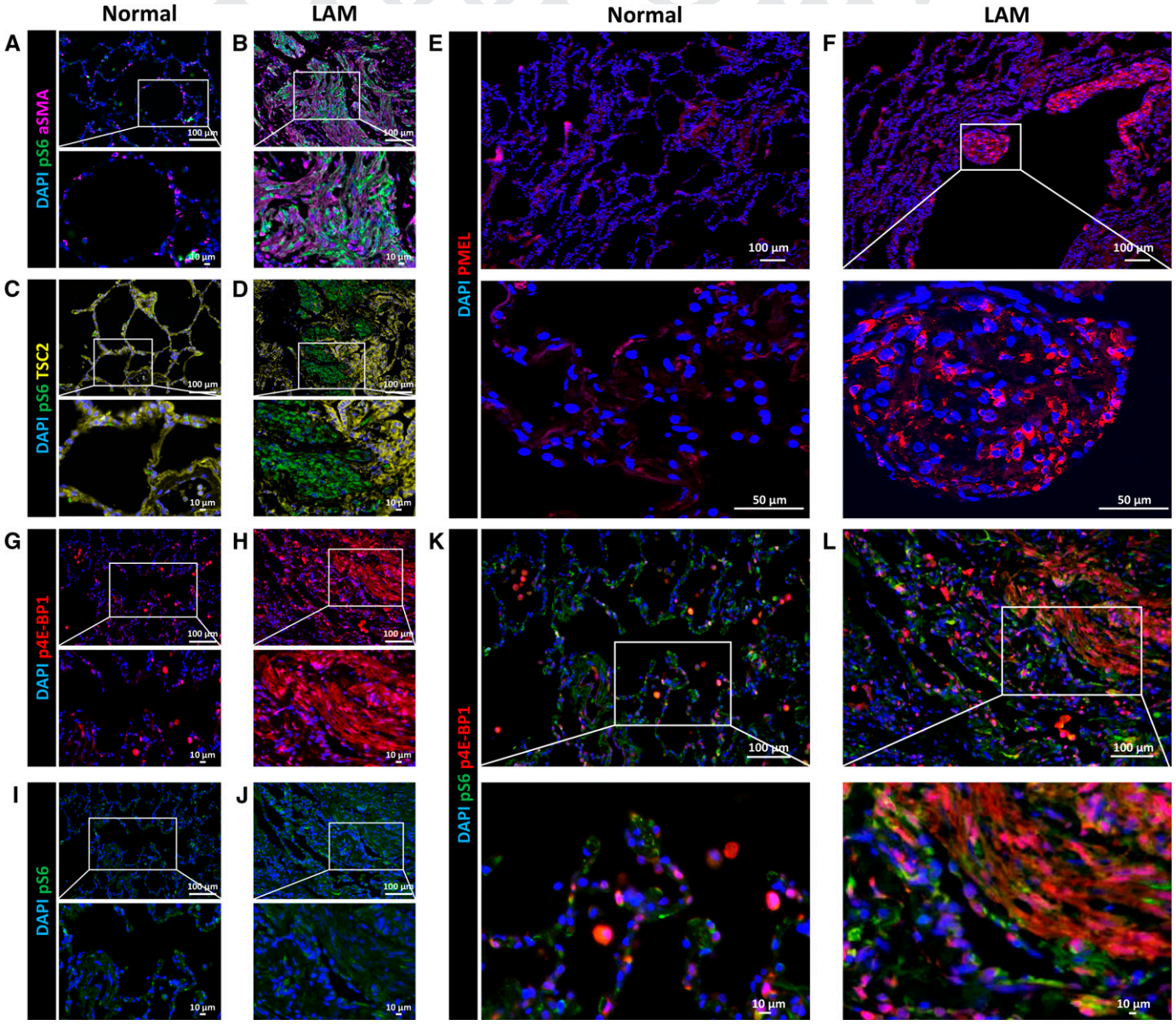

Figure 2. Immunofluorescent expression of pS6 and p4E-BP1 in normal and LAM lung. (*A* and *B*) pS6 (green) and α-SMA (purple pseudocolor) in normal (*A*) and LAM (*B*) lung alveoli. (*C* and *D*) pS6 (green), Tsc2/tuberin (yellow pseudocolor) in normal (*C*) and LAM (*D*) lung alveoli. (*E* and *F*) PMEL (red) in normal (*E*) and LAM (*F*) lung. (*G* and *H*) p4E-BP1 (red pseudocolor) in normal (*G*) and LAM (*H*) lung. (*I* and *J*) pS6 (green) in normal (*I*) and LAM (*J*) lung. (*K* and *L*) pS6 (green), p4E-BP1 (red pseudocolor) immunofluorescent costaining in normal (*K*) and LAM (*L*) lung. Immunofluorescent protein expression was studied in three different normal lungs and three different LAM lungs. Scale bars indicate range from 10 μm to 100 μm, depending on image magnification. DAPI (blue) staining in all subfigures and immunofluorescent staining were performed as described in Methods.

research has suggested that Tsc2-positive myofibroblast cells are a significant proportion of cells within advanced LAM lung lesions (29). We performed *in vitro* studies in LAFs derived from patients with LAM undergoing lung transplantation and, although there is heterogeneity of expression between different primary LAF cell lines, they predominantly express full-length Tsc2/tuberin (30) (Figure E2). Such LAFs have successfully been grown *in vitro* for at least six passages and, in some, Tsc2 mutations have been determined (22). In our laboratory, NHLFs and LAFs generally have similar protein expression of Tsc2/tuberin, pS6, p4E-BP1, and eIF4E protein (Figure E2). Primary lung LAFs are the only available human lung LAM cells for *in vitro* studies and reflect most fibroblasts in the LAM lung as opposed to immortalized cell lines.

In fibroblasts from normal or LAM lungs, we demonstrated growth inhibition by the cytostatic mTORC1 inhibitor rapamycin, the cytotoxic bi-steric inhibitor RMC-5552, and the dual mTORC1/mTORC2 kinase inhibitors Torin 1 and INK128 (Figures 3A and 3B). Both rapamycin and RMC-5552

were potent subnanomolar inhibitors of growth of NHLFs and LAFs (IC50s ~0.2 nM), whereas Torin 1 and INK128 were ~10-fold less potent (IC50s ~2.5 nM). All growth inhibition shown in Figure 3, except for that with the allosteric, cytostatic inhibitor rapamycin, resulted in less than the original seeded number of cells, illustrating some cytotoxic activity. This cytotoxicity is likely to be due to apoptosis, as has been previously shown for other bi-steric inhibitors in mouse and human cancer cells and in mouse embryonic fibroblasts (19).

To address the durability of inhibition of growth of LAFs by rapamycin versus RMC-5552 we performed three separate drug washout/regrowth experiments in LAFs from three different patients (Figures 3C and 3D). After drug treatment, growth of rapamycin or RMC-5552–treated cells was compared with nontreated LAF growth after 7 days. No appreciable growth was seen in rapamycin or RMC-5552–treated cells. A second plate was seeded at the same time as plate 1, with duplicate or triplicate drug-treated wells but no control cells, and after the first growth period, the drug-treated wells were washed out and cells cultured in medium. After 6 days of regrowth, rapamycin-treated cells were confluent, but there was minimal growth in the RMC-5552–treated cells, attesting to the effective durable inhibition of LAF growth by RMC-5552 in contrast to rapamycin (Figures 3C and 3D). Similar results were demonstrated *in vivo* with rapamycin-treated tumors regrowing rapidly versus much slower regrowth of tumors treated with bi-steric inhibitors (19).

mTORC1/mTORC2 Protein Phosphorylation Signaling Profiles after Treatment with Inhibitors

We next examined the inhibition of mTORC1 and mTORC2 protein phosphorylation signaling by rapamycin (10 nM), RMC-5552 (10 nM), and two dual TOR kinase inhibitors Torin 1 (100 nM) and INK128 (100 nM) in different LAF cell lines. Representative immunoblots of the phosphorylation by mTORC1 of pS6 and p4E-BP1 and by mTORC2 of pAkt and pNDGR1 are shown in Figures 4A–4D. Expression of total nonphosphorylated proteins was consistent across gels (Figures 4A and 4C). RMC-5552 and the mTOR kinase active site inhibitors prevented phosphorylation of both pS6 and p4E-BP1, whereas rapamycin only inhibited pS6. Neither RMC-5552 nor rapamycin inhibited pAkt and pNDGR1, indicating that, at this concentration, they were both selective for mTORC1 (Figure 4). 4E-BP1 has at least six phosphorylation sites, and two-dimensional gel electrophoresis has shown that Thr37/46 and S65/Thr70 can be phosphorylated by mTORC1 (30). However, only the

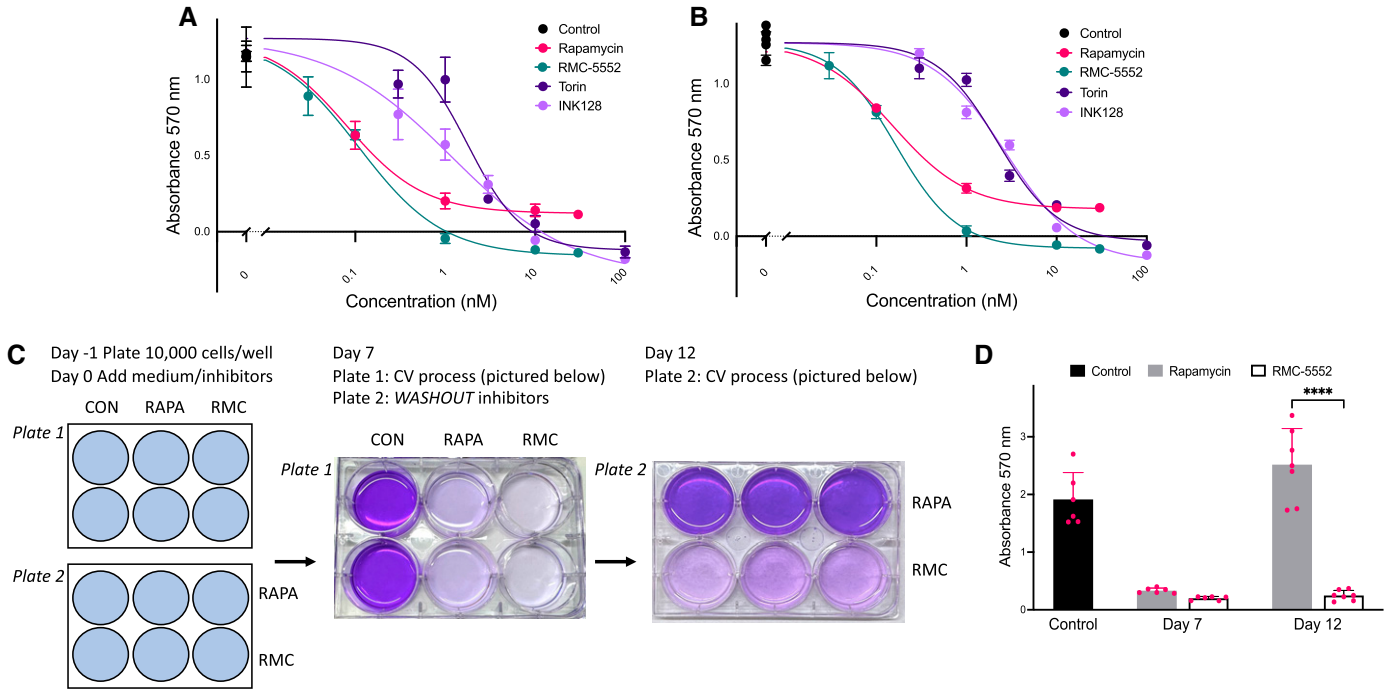

Figure 3. Normal and LAM-associated lung fibroblast growth inhibition studies. (*A* and *B*) Normal human lung fibroblasts (NHLFs) or LAM-associated fibroblasts (LAFs) were grown in the presence or absence of drugs and growth determined 72 hours after drug treatment. Growth curves from one NHLF and one LAF cell line represent similar results from three different NHLF lung lines and three different patients with LAM LAF cell lines. All drug treatments were in quadruplicate and compared with 20 control readings. Growth inhibition curves were produced using a variable slope (four parameter) nonlinear regression analysis initialized to mean of respective controls with a 95% confidence interval. Quantitative data are presented as mean ± SEM. (*C*) LAFs were seeded at 10,000 cells/well in plates 1 and 2. Plate 1 was treated with control (CON; 0.1% DMSO), rapamycin (RAPA; 10 nM), or RMC-5552 (RMC; 10 nM). In plate 2, wells were treated in duplicate or triplicate with rapamycin (10 nM) or RMC-5552 (10 nM). Fresh medium plus or minus drugs was added every 2–3 days to plates 1 and 2 for 7 days when plate 1 controls were confluent and growth was determined by crystal violet (CV) staining as described in Methods. In plate 2, drug-treated cells were washed twice with DPBS, fresh medium added, and grown for another 6 days. (*D*) Washout data from three similar experiments with three separate LAF cells lines were pooled. Quantitative graph data are represented as mean ± SD and *P* values determined by Tukey two-way ANOVA, where $^{*}P < 0.05$, $^{**}P < 0.01$, $^{***}P < 0.001$, and $^{****}P < 0.0001$.

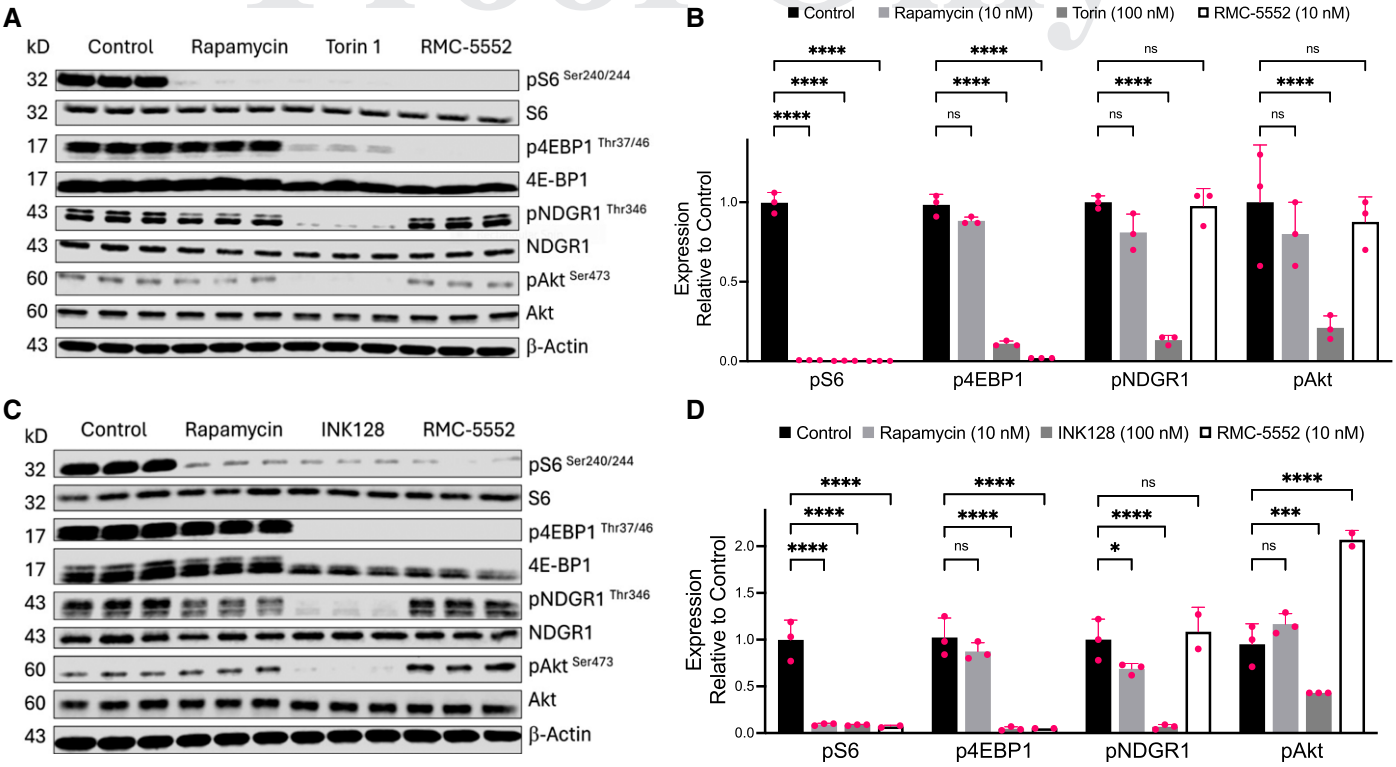

Figure 4. Inhibition of mTOR (mammalian target of rapamycin) signaling in LAFs. (*A*) Immunoblot of phosphorylated proteins in one LAF cell line. Control (0.1% DMSO), Rapamycin (10 nM), Torin 1 (100 nM), RMC-5552 (10 nM) for pS6$^{Ser240/244}$, S6, p4E-BP1, 4E-BP1 (mTORC1), pAkt^{Ser473}, Akt, pNDGR1^{Thr346}, NDGR1 (mTORC2), and β-Actin. (*B*) Quantitation (Prism) of phosphorylation of proteins in *A*. (*C*) Immunoblot of phosphorylated proteins in a second LAF cell line, as described in *A*, with same treatments as *A* except INK128 (100 nM) in place of Torin 1 (100 nM). (*D*) Quantitation of phosphorylated proteins in *C*. Data are representative of those obtained with three separate LAF cell lines. Immunoblot protein bands were quantitated on an Odyssey LiCor reader, with each band's intensity normalized to β-Actin in that lane, then graphed relative to average of triplicate (except for one duplicate in pAkt in *C*), and each drug-treated band compared with its respective control band set as 1.0. Error bars are represented as mean ± SD and *P* values determined by Tukey two-way ANOVA, where $^{*}P<0.05$, $^{**}P<0.01$, $^{***}P<0.001$, and $^{****}P<0.0001$.

rapamycin-insensitive phosphorylation of p4E-BP1 Thr37/46, the site we studied here, results in the release of eIF4E (11).

Immunofluorescent Expression of p4E-BP1 in Untreated LAFs or LAFs Treated with Inhibitors

We investigated the immunofluorescent expression of p4E-BP1 Thr37/46 protein in control or rapamycin (10 nM), INK128 (100 nM), or RMC-5552 (10 nM)–treated LAFs (Figure 5). In control LAFs, p4E-BP1 was highly expressed in nuclei with less intensity in cytoplasm (Figure 5A). This was somewhat unexpected, because the majority of mTORC1 studies have emphasized the expression of mTORC1 activity on lysosomes in the cytoplasm (7). It is possible, but unlikely, that p4E-BP1 was translocated from the cytoplasm to the nucleus. However, nuclear nonphosphorylated 4E-BP1 and mTOR activity has been reported previously (9). As expected, rapamycin did not significantly inhibit p4E-BP1, whereas both RMC-5552 and INK128 greatly reduced both nuclear and cytoplasmic p4E-BP1 expression (Figures 5B–5E).

Discussion

Activation of cell growth by the mTORC1 pathway is mainly achieved via an increase of mRNA translation through the S6K/S6 and 4E-BP1/eIF4E axes (Figure E1A). Translation initiation of m7G-capped mRNAs requires preassembly of the eIF4F complex made up of the cap binding protein eIF4E; the scaffold protein eIF4G, which competes with 4E-BP for binding eIF4E; and eIF4A, an RNA helicase, which unwinds complex secondary 5′ structure (9) (Figure E1C). The mTORC1-driven eIF4E translation initiation axis is overexpressed in many cancers but is not essential for physiologically expressed genes, and the heterozygous deletion of eIF4E in mice causes no phenotypic changes (31). However, "weak" mRNAs, such as c-Myc, cyclin D1, Bcl2, TFEB, and ESR1, are dependent on increased expression of eIF4E (31). We have previously suggested that the rapamycin-insensitive eIF4E-dependent translation initiation pathway is a neglected target in LAM (32). In this study, we analyzed the expression of the eIF4E-dependent translation initiation genes in unique LAM lung cell clusters based on their expression of 55 cancer stem cell genes (25). The expression of the eIF4F complex translation initiation genes was highest in the SLS cluster of LAM cells, whereas the 4E-BP1 gene was least expressed in the SLS cluster. This suggested that the SLS cells have the capacity for unrestrained 4E-BP1/eIF4E

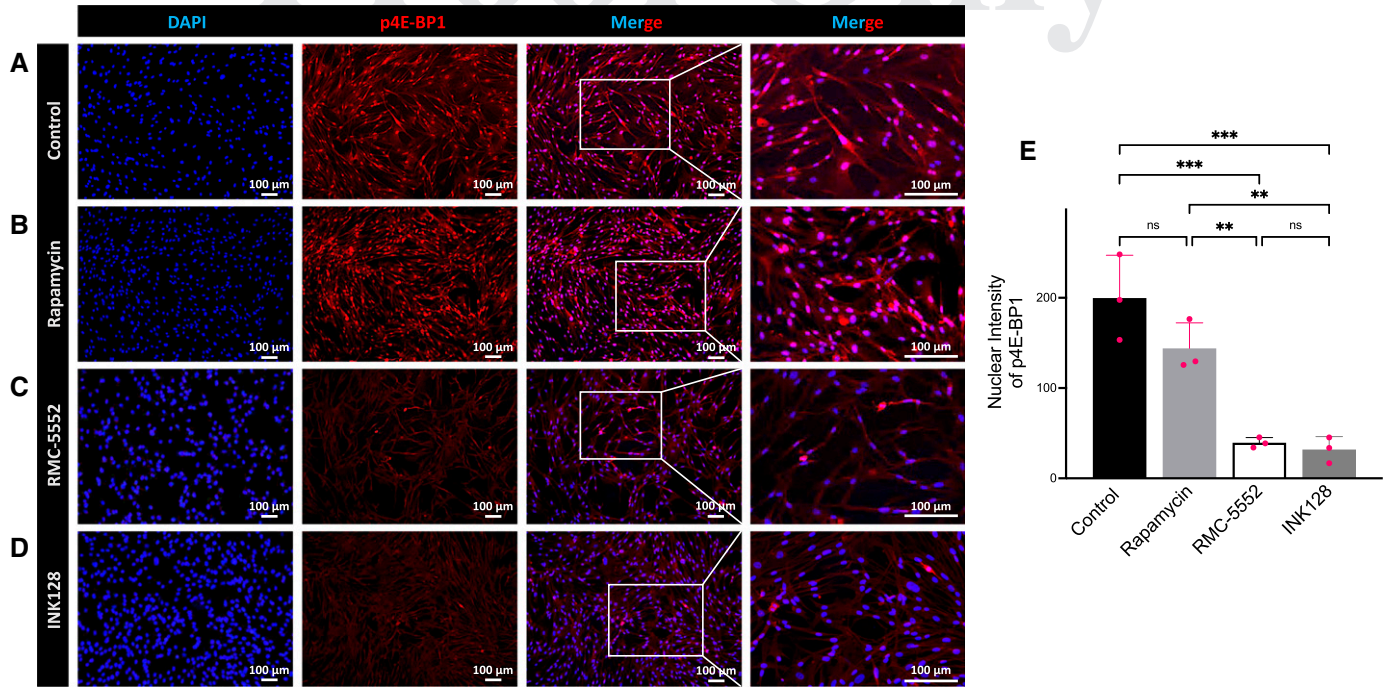

Figure 5. Immunofluorescent analysis of expression of p4E-BP1 protein in LAFs. (*A*) Control- (0.1% DMSO), (*B*) rapamycin- (10 nM), (*C*) RMC-5552– (10 nM), and (*D*) INK128- (100 nM) treated LAFs. Cells from one LAF line were plated at 50,000 cells/well in the presence or absence of drugs on chamber slides and grown for 20 hours in 10% FBS medium. Cells were then fixed, incubated with antibodies for 1 hour at room temperature, stained, washed, and embedded in ProLong Diamond embedding media. All panels were at a scale of 100 μm except the right panel, where the scale was 10 μm, as indicated by their respective scale bars. (*E*) Graph of nuclear expression of p4E-BP1. Quantification of nuclear p4E-BP1 fluorescence from three representative images, counting more than 250 cells per condition. Cell nuclei were identified with the ImageJ (2.14.0) "Threshold" function, with subsequent "Analyze Particles" and measurements taken to quantify nuclear intensity of p4E-BP1 signal. Error bars are represented as mean ± SD and *P* values determined by Tukey two-way ANOVA, where $*P < 0.05$, $**P < 0.01$, and $***P < 0.001$.

oncogenic mRNA translation inhibition. The LAM SLS cluster also expressed dormancy and resistance genes; immune suppressive genes; and angiogenic, ECM remodeling, and estrogen sensitivity genes (23), as seen in cancer stem cells (33). However, to our knowledge, there has been no study of 4E-BP1 or the eIF4F complex (eIF4E, eIF4G, eIF4A) gene expression in any other cancer stem cells. ESR1 has been shown to be expressed in the SLS LAM cells (23) and is required for breast cancer cells to enter dormancy (34). Estrogen increased angiomyolipoma cell proliferation, and LAM disease is often identified or exacerbated during pregnancy (35). In an LAM genome-wide association study, the NR2F2 (nuclear receptor subfamily 2 group F member 2) stemness transcription factor was linked to disease (36). A closely related nuclear transcription family member, NR2F1, was identified in the SLS cluster in LAM lung (23). NR2F1 is an orphan nuclear receptor of the steroid/thyroid hormone receptor superfamily and is a master regulator of tumor cell dormancy (37). Both NR2F1 and NF2R2 were found in another study in the top 1% of transcription factor genes in an LAM core transcriptional regulatory network (38). The expression of ESR1 and NR2F1 stemness transcription factors in SLS LAM cells with low 4E-BP1 and high eIF4E expression is supportive of the hypothesis that this axis of mTORC1 activation is critical for LAM cell survival.

Our novel hypothesis, which needs further research to be verified, is that ESR1/NR2F1/eIF4E–expressing SLS LAM cells are estrogen-responsive progenitors of the IS LAM cells, and RMC-5552, but not rapamycin, destroys SLS cells, thereby also reducing IS cells (Figure E2). The surrounding LAFs provide a supportive lung microenvironment for growth of both SLS and IS LAM cells and would also be inhibited by rapamycin and RMC-5552 (Figure E3). We performed our *in vitro* studies in LAFs derived from LAM lung tissue from patients with advanced LAM disease in whom it is likely that Tsc2-expressing LAFs make up a significant portion of lesions (29, 45).

Bi-steric mTORC1-selective inhibitors were developed to be superior, more durable cell growth inhibitors than rapamycin and to prevent some of the toxicities of inhibition of mTORC2 by dual mTOR kinases inhibitors (16–18). As expected, we observed effective growth inhibition by rapamycin and RMC-5552 in both NHLFs and LAFs. The similarity of expression of Tsc2/tuberin in NHLFs and LAFs is a limitation of the use of LAFs *in vitro* as representative of unique Tsc2-null LAM cells, in which these inhibitors might have a greater growth inhibition potency. A detailed previous study proved that the bi-steric inhibitors RMC-5552, RMC-4627, and RMC-6272 inhibited growth of patient-derived xenografts *in vivo* (19). All *in vitro* experiments in this manuscript were with the nonclinical RMC-4627 and RMC-6272, which demonstrated a modest increase in potency for growth inhibition of TSC-negative over TSC-expressing tumor cells (19). However, like our results, cell proliferation was blocked by the bi-steric inhibitors for longer than rapamycin (19).

The study of bi-steric inhibitors in tumor cells also demonstrated global rewiring of cellular metabolism and importantly, in contrast to rapamycin, enhanced cancer cell apoptosis (19). In a separate publication, mTORC1 activity has been shown to oscillate throughout the cell cycle, peaking in S and G2 and lowest in mitosis and G1 (20). These authors demonstrated that rapamycin mainly blocked the cell cycle at the G2-mitosis checkpoint, whereas RMC-5552 inhibited both S phase and G2. In yet another publication, RMC-6272 blocked 4E-BP1 phosphorylation, reduced the prosurvival protein MCL1, and had increased efficacy over the rapamycin analog RAD001 (Everolimus) in ER+/HER2− breast cancer hormone therapy–resistant cell lines versus their parental lines (39).

16

Our immunofluorescent studies in LAM lung showed that pS6 and p4E-BP1 expression overlaps with some α-SMA–positive cells in LAM lung, consistent with the heterogeneity of myofibroblast-like cells in LAM lesions. The LAM lung-specific protein PMEL showed only a proportion of LAM nodule cells express this marker. Together with *bona fide* TSC-null LAM cells, LAFs influence the behavior of surrounding epithelial, endothelial, and immune cells (21–23, 30). In lung myofibroblasts and NHLFs, the bi-steric inhibitor Rapalink-1 prevented metabolic reprogramming downstream of TGF-β, whereas rapamycin had no effect (46). The rapamycin-insensitive, mTORC1 4E-BP/eIF4E axis, but not mTORC2 activation, was also critical for fibrogenesis in idiopathic pulmonary fibroblasts (47). We did not investigate TGF-β signaling in the present study, but we have previously observed increased expression of ECM genes, including TGF-β2 and TGF-β3, in LAM lung cells (22). Cancer stem cells are often found on the surface of tumors and are protected by ECM and cancer-associated fibroblasts, which are known to have high plasticity in tumor environments (35). It is possible in the future that detailed spatial transcriptomic studies might be able to detect the exact location of the SLS LAM cells in LAM lesions.

In our current study, we were somewhat surprised by the prominent expression of p4E-BP1 in the nuclei of LAFs. However, the presence of both the p70 and p85 isoforms of pS6K1 has been previously reported in the nucleus of other cells (40). Other research in mouse embryo fibroblasts and other cells has shown ∼30% of the nonphosphorylated 4E-BP1 itself is nuclear and ∼70% cytoplasmic (9), but the cellular distribution of p4E-BP1 in LAM lung or LAFs has not been previously described. In addition to cytoplasmic translation initiation, eIF4E functions as a nuclear mRNA exporter and nuclear mRNA splicer (41–44). Differential analysis of the phosphoproteome of Tsc2-null 705 cells demonstrated that proteins involved in ribonucleoprotein biogenesis, ribosome biogenesis, and RNA splicing were the most downregulated by the bi-steric inhibitor RMC-6272 versus rapamycin (19). In addition, 400 genes were identified by scRNA-seq that had differential alternative RNA splicing induced by RMC-6272 versus rapamycin (19). Our immunofluorescent studies suggest that mTORC1 phosphorylation of p4E-BP1 is likely to occur in the nucleus in LAM lesions and in LAFs grown *in vitro* and suggests that there may be other important, undiscovered mTORC1 nuclear roles in LAM.

In other research, rapamycin has been shown to potently block the S6K1/S6 ribosomal synthesis pathway, but not phosphorylation of 4E-BP1 Thr37/46, even at concentrations 100-fold higher than clinically measured in patients with LAM on a standard 2 mg/d dosage (5, 48). It should be noted that, although no human tissue distribution is available for rapamycin, in rats the drug is found in lung and liver at ∼30-fold over blood concentrations (49), but it is unlikely in human lung to reach 100-fold over blood concentrations. This suggests that in patients with LAM treated with rapamycin, there is incomplete inhibition of the 4E-BP1/eIF4E pathway in the lung. In late-stage LAM disease, the lung architecture has large cystic spaces and nodules, suggesting that stronger interventions than rapamycin might be required to treat advanced LAM or rapamycin-insensitive disease.

RMC-5552 is the only bi-steric mTORC1-selective inhibitor in clinical trials, and it has shown some effectiveness in patients with cancer with mutations in the PI3K/mTOR pathways (50). In many patients with LAM, the use of rapamycin has resulted in patients having a chronic disease. However, on cessation of the drug, the disease returns, and with long-term use many patients become resistant to rapamycin and require lung transplant. We propose that RMC-5552 has the potential to eradicate LAM SLS cells, thereby offering a treatment option that could be administered intermittently, with potentially fewer adverse effects than rapamycin, which must be administered continuously. ■

Author disclosures are available with the text of this article at www.atsjournals.org.

Acknowledgment: The authors thank patients with lymphangioleiomyomatosis who contributed tissues for these studies, the National Disease Research Institute for collecting and distributing these samples, Professors Nahum Sonenberg and Marina Holz for helpful discussions, John Hutchinson for chemical structures, and Kevin Clark for the exquisite cartoons. The authors thank the Pathology Core Laboratory of the Children's Hospital of Philadelphia Research Institute and the Specialized Histopathology Core at the Boston Dana/Farber/Harvard Cancer Centre for providing histology services.

References

1. Carsillo T, Astrinidis A, Henske EP. Mutations in the tuberous sclerosis complex gene TSC2 are a cause of sporadic pulmonary lymphangioleiomyomatosis. *Proc Natl Acad Sci U S A* 2000;97: 6085–6090.
2. Goncharova EA, Goncharov DA, Eszterhas A, Hunter DS, Glassberg MK, Yeung RS, *et al.* Tuberin regulates p70S6 kinase activation and ribosomal protein S6 phosphorylation: a role for the TSC2 tumor suppressor gene in pulmonary lymphangioleiomyomatosis (LAM). *J Biol Chem* 2002;277:30958–30967.
3. McCarthy C, Gupta N, Johnson SR, Jane JY, McCormack FX. Lymphangioleiomyomatosis: Pathogenesis, clinical features, diagnosis, and management. *Lancet Respir Med* 2021;9:1313–1327.
4. McCormack FX, Travis WD, Colby TV, Henske EP, Moss J. Lymphangioleiomyomatosis. Calling it what it is: a low-grade, destructive, metastasizing neoplasm. *Am J Respir Crit Care Med* 2012;186: 1210–1212.
5. McCormack FX, Inoue Y, Moss J, Singer LG, Strange C, Nakata K, *et al.*; MILES Trial Group. Efficacy and safety of sirolimus in lymphangioleiomyomatosis. *N Engl J Med* 2011;364: 1595–1606.

6. Battaglioni S, Benjamin D, Wälchli M, Maier T, Hall MN. mTOR substrate phosphorylation in growth control. *Cell* 2022;185:1814–1836.
7. Saxton RA, Sabatini DM. mTOR signaling in growth, metabolism, and disease. *Cell* 2017;168:960–976.
8. Pelletier J, Sonenberg N. Therapeutic targeting of eukaryotic initiation factor (eIF) 4E. *Biochem Soc Trans* 2023;51:113–124.
9. Rong L, Livingstone M, Sukarieh R, Petroulakis E, Gingras A-C, Crosby K, *et al.* Control of eIF4E cellular localization by eIF4E-binding proteins, 4E-BPs. *RNA* 2008;14:1318–1327.
10. Gingras A-C, Gygi SP, Raught B, Polakiewicz RD, Abraham RT, Hoekstra MF, *et al.* Regulation of 4E-BP1 phosphorylation: a novel two-step mechanism. *Genes Dev* 1999;13:1422–1437.
11. Böhm R, Imseng S, Jakob RP, Hall MN, Maier T, Hiller S. The dynamic mechanism of 4E-BP1 recognition and phosphorylation by mTORC1. *Mol Cell* 2021;81:2403–2416.e5.
12. Ducker GS, Atreya CE, Simko JP, Hom YK, Matli MR, Benes CH, *et al.* Incomplete inhibition of phosphorylation of 4E-BP1 as a mechanism of primary resistance to ATP-competitive mTOR inhibitors. *Oncogene* 2014;33:1590–1600.
13. Evans JF, Rue RW, Mukhitov AR, Obraztsova K, Smith CJ, Krymskaya VP. Inhibition of growth of TSC2-null cells by a PI3K/mTOR inhibitor but not by a selective MNK1/2 inhibitor. *Biomolecules* 2019;10:28.
14. Hagiwara A, Cornu M, Cybulski N, Polak P, Betz C, Trapani F, *et al.* Hepatic mTORC2 activates glycolysis and lipogenesis through AKT, glucokinase, and SREBC1. *Cell Metab* 2012;15:725–738.
15. Rodrik-Outmezguine VS, Okaniwa M, Yao Z, Novotny CJ, McWhirter C, Banaji A, *et al.* Overcoming mTOR resistance mutations with a new-generation mTOR inhibitor. *Nature* 2016;534:272–276.
16. Lee BJ, Mallya S, Dinglasan N, Fung A, Nguyen T, Herzog LO, *et al.* Efficacy of a novel bi-steric mTORC1 inhibitor in models of B-cell acute lymphoblastic leukemia. *Front Oncol* 2021;11:673213.
17. Lee BJ, Boyer JA, Burnett GL, Thottumkara AP, Tibrewal N, Wilson SL, *et al.* Selective inhibitors of mTORC1 activate 4EBP1 and suppress tumor growth. *Nat Chem Biol* 2021;17:1065–1074.
18. Burnett GL, Yang YC, Aggen JB, Pitzen J, Gliedt MK, Semko CM, *et al.* Discovery of RMC-5552, a selective bi-steric inhibitor of mtorc1, for the treatment of mTORC1-activated tumors. *J Med Chem* 2023;66: 149–169.
19. Du H, Yang YC, Liu H-J, Yuan M, Asara JM, Wong K-K, *et al.* Bi-steric mTORC1 inhibitors induce apoptotic cell death in tumor models with hyperactivated mTORC1. *J Clin Invest* 2023;133:e167861.
20. Mahauad-Fernandez WD, Yang YC, Lai I, Park J, Yao L, Evans JW, *et al.* Bi-steric mTORC1-selective inhibitors activate 4E-BP1 reversing myc-induced tumorigenesis and synergize with immunotherapy [preprint]. *bioRxiv*; 2022 [accessed ■■■]. Available from: https://www.biorxiv.org/content/10.1101/2022.02.04.478208v1.
21. Guo M, Yu JJ, Perl AK, Wikenheiser-Brokamp KA, Riccetti M, Zhang EY, *et al.* Single-cell transcriptomic analysis identifies a unique pulmonary lymphangioleiomyomatosis cell. *Am J Respir Crit Care Med* 2020;202: 1373–1387.
22. Obraztsova K, Basil MC, Rue R, Sivakumar A, Lin SM, Mukhitov AR, *et al.* mTORC1 activation in lung mesenchyme drives sex-and age-dependent pulmonary structure and function decline. *Nat Commun* 2020;11:5640.
23. Tang Y, Kwiatkowski DJ, Henske EP. Midkine expression by stem-like tumor cells drives persistence to mTOR inhibition and an immune-suppressive microenvironment. *Nat Commun* 2022;13:5018.
24. Du Y, Guo M, Wu Y, Wagner A, Perl AK, Wikenheiser-Brokamp K, *et al.* Lymphangioleiomyomatosis (LAM) cell atlas. *Thorax* 2023;78:85–87.
25. Yuan H, Yan M, Zhang G, Liu W, Deng C, Liao G, *et al.* CancerSea: a cancer single-cell state atlas. *Nucleic Acids Res* 2019;47:D900–D908.
26. Alain T, Morita M, Fonseca BD, Yanagiya A, Siddiqui N, Bhat M, *et al.* eIF4E/4E-BP ratio predicts the efficacy of mTOR targeted therapies. *Cancer Res* 2012;72:6468–6476.
27. Qin X, Jiang B, Zhang Y. 4E-BP1, a multifactor regulated multifunctional protein. *Cell Cycle* 2016;15:781–786.
28. Matsumoto Y, Horiba K, Usuki J, Chu SC, Ferrans VJ, Moss J. Markers of cell proliferation and expression of melanosomal antigen in lymphangioleiomyomatosis. *Am J Respir Cell Mol Biol* 1999;21: 327–336.
29. Clements D, Dongre A, Krymskaya VP, Johnson SR. Wild type mesenchymal cells contribute to the lung pathology of lymphangioleiomyomatosis. *PLoS One* 2015;10:e0126025.
30. Lin SM, Rue R, Mukhitov AR, Goel A, Basil MC, Obraztsova K, *et al.* Hyperactive mTORC1 in lung mesenchyme induces endothelial cell dysfunction and pulmonary vascular remodeling. *J Clin Invest* 2023; 134:e172116.
31. Truitt ML, Conn CS, Shi Z, Pang X, Tokuyasu T, Coady AM, *et al.* Differential requirements for eIF4E dose in normal development and cancer. *Cell* 2015;162:59–71.
32. Evans JF, McCormack FX, Sonenberg N, Krymskaya VP. Lost in translation: a neglected mTOR target for lymphangioleiomyomatosis. *Eur Respir Rev* 2023;32:230100.
33. Aouad P, Zhang Y, De Martino F, Stibolt C, Ali S, Ambrosini G, *et al.* Epithelial-mesenchymal plasticity determines estrogen receptor positive breast cancer dormancy and epithelial reconversion drives recurrence. *Nat Commun* 2022;13:4975.
34. Yu J, Astrinidis A, Howard S, Henske EP. Estradiol and tamoxifen stimulate LAM-associated angiomyolipoma cell growth and activate both genomic and nongenomic signaling pathways. *Am J Physiol Lung Cell Mol Physiol* 2004;286:L694–L700.
35. Liu Q, Guo Z, Li G, Zhang Y, Liu X, Li B, *et al.* Cancer stem cells and their niche in cancer progression and therapy. *Cancer Cell Int* 2023;23:305.
36. Kim W, Giannikou K, Dreier JR, Lee S, Tyburczy ME, Silverman EK, *et al.* A genome-wide association study implicates NR2F2 in lymphangioleiomyomatosis pathogenesis. *Eur Respir J* 2019;53:1900329.
37. Khalil BD, Sanchez R, Rahman T, Rodriguez-Tirado C, Moritsch S, Martinez AR, *et al.* An NR2F1-specific agonist suppresses metastasis by inducing cancer cell dormancy. *J Exp Med* 2022;219:e20210836.
38. Olatoke T, Wagner A, Astrinidis A, Zhang EY, Guo M, Zhang AG, *et al.* Single-cell multiomic analysis identifies a HOX-PBX gene network regulating the survival of lymphangioleiomyomatosis cells. *Sci Adv* 2023;9:eadf8549.
39. Meng D, Zhao X, Yang YC, Navickas A, Helland C, Goodarzi H, *et al.* A bi-steric mTORC1-selective inhibitor overcomes drug resistance in breast cancer. *Oncogene* 2023;42:2207–2217.
40. Torres AS, Holz MK. Unraveling the multifaceted nature of the nuclear function of mTOR. *Biochim Biophys Acta Mol Cell Res* 2021;1868: 118907.
41. Giguere V. Canonical signaling and nuclear activity of mTOR-a teamwork effort to regulate metabolism and cell growth. *FEBS J* 2018;285: 1572–1588.
42. Zhou X, Zhong Y, Zhang J. Regulation of nuclear mTORC1. *Mol Cell Oncol* 2021;8:1896348.
43. Zhao T, Fan J, Abu-Zaid A, Burley SK, Zheng, XFS. Nuclear mTOR signaling orchestrates transcriptional programs underlying cellular growth and metabolism. *Cells* 2024;13:781.
44. Mars JC, Culjkovic-Kraljacic B, Borden KLB. eIF4E orchestrates mRNA processing, RNA export and translation to modify specific protein production. *Nucleus* 2024;15:2360196.
45. Miller S, Stewart ID, Clements D, Soomro I, Babaei-Jadidi R, Johnson SR. Evolution of lung pathology in lymphangioleiomyomatosis: associations with disease course and treatment response. *J Pathol Clin Res* 2020;6:215–226.
46. O'Leary EM, Tian Y, Nigdelioglu R, Witt LJ, Cetin-Atalay R, Meliton AY, *et al.* TGF-β promotes metabolic reprogramming in lung fibroblasts *via* mTORC1-dependent ATF4 activation. *Am J Respir Cell Mol Biol* 2020; 63:601–612.
47. Woodcock HV, Eley JD, Guillotin D, Platé M, Nanthakumar CB, Martufi M, *et al.* The mTORC1/4E-BP1 axis represents a critical signaling node during fibrogenesis. *Nat Commun* 2019;10:6.
48. Mortensen DS, Fultz KE, Xu S, Xu W, Packard G, Khambatta G, *et al.* CC-223, a potent and selective inhibitor of mTOR kinase*: In vitro* and *in vivo* characterization. *Mol Cancer Ther* 2015;14:1295–1305.
49. Napoli KL, Wang ME, Stanislaw M, Stepkowski SM, Kahan BD. Distribution of sirolimus in rat tissue. *Clin Biochem* 1997;30:135–142.
50. Schram AM, Naqash AR, Haura EB, Riess JW, Ulahannan SV, Ou S-HI, *et al.* First-in-human phase 1/1b trial of the first-in-class bi-steric mTORC1-selective inhibitor RMC-5552 in patients with advanced solid tumors [abstract]. *Mol Cancer Ther* 2023;22:C020.

AUTHOR QUERIES

Please check all figure text, labels, and legends for accuracy and completeness.

QA1 If you provided an ORCID ID at submission, please confirm that it appears correctly on the opening page of this article.

QA2 Please confirm that all necessary grants and funding sources are mentioned in the support footnote.

1 Per journal style, affiliations must appear in numeric order, which may require out-of-order numbering in the author line. The affiliations have been grouped according to top-level institution and location, as necessary. Please confirm edits to the affiliations and corresponding author line numbering.

2 Per journal style, each affiliation may appear in either English or the language spoken at the location of the affiliation. However, each affiliation should be entirely one language. Please choose one language and edit affiliation 5 as necessary.

3 Please spell out UMR, INRAE, and ERN-LUNG in the affiliations, unless the abbreviation is part of the official name of the institution.

4 Please confirm edit of initials from S.W.K. to S.V.K. to match author list.

5 Per journal style, author disclosures of potential conflicts of interest should appear online and have been deleted here. Please confirm that this information has been provided to the ATS editorial office on the appropriate forms.

6 Please check slashes throughout and replace with "and", "or", or "and/or" if appropriate.

7 Any variations in capitalization and/or italics in genetic nomenclature have been retained per the original manuscript. Please confirm that all nomenclature has been formatted properly throughout. Per journal style, gene and protein symbols should be explained parenthetically after the symbol and defined in figures and table legends. However, if a gene/protein is mentioned in passing or is peripheral to the main point/discussion, it is not necessary to add an explanation. Also, these symbols may be retained even if used only once, and they do not need to be defined in titles. Please verify appropriate use throughout.

8 Please confirm the changes to the sentence beginning "Rapamycin inhibits" retain your intended meaning

9 Please confirm the changes to the sentence beginning "These two compounds" retain your intended meaning.

10 Please check use of "immunofluorescent" and "immunofluorescence" throughout and confirm that these have been used consistently as intended.

11 Please confirm expansion of IRB at both occurrences in the text.

12 Please confirm expansion of NIH at only use in text.

13 Please confirm expansion of DMEM at only use in text.

14 Please confirm expansion of RT at both occurrences in the text and Figure 5 legend.

15 Please confirm the changes to the sentence beginning "The LAM SLS cluster" retain your intended meaning.

16 Reference citations are not in sequential order. Please check and reorder accordingly.

17 For Reference 20, please provide the date you accessed the article.

18 Please confirm that all figures are original to this manuscript and have not previously appeared elsewhere in any print or electronic form (including the Internet). If they have appeared elsewhere, please provide the reference of the source, as well as confirmation that written permission to reprint (or reprint with modifications) has been received (or that the original is in the public domain). If the original is an ATS publication, permission is automatically granted.

19 Please confirm crystal violet is correct expansion for CV in Figure 3 legend.

20 Please spell out DPBS at only use in text.